Electronic Supplementary Information

Fluorescent probe for selective detection of boric acids and its application to screening the conversion of Suzuki-Miyaura coupling reaction

Min Sik Eom†, Byoung Yong Park†, Seungyoon Kang† and Min Su Han*

Department of Chemistry, Gwangju Institute of Science and Technology (GIST), 123 Cheomdangwagi-ro, Buk-gu, Gwangju 61005, Republic of Korea

* E-mail: happyhan@gist.ac.kr

† Min Sik Eom, Byoung Yong Park and Seungyoon Kang contributed equally to this work.

Table of Contents

S.1. General Information

Unless stated otherwise, all reactions were carried out under atmospheric environment.

All chemical reagents were purchased from Sigma-Aldrich, Tokyo Chemical Industry (TCI), Alfa Aesar, Daejung Chemical Industry and Duksan. Unless otherwise stated, they were used without further purification. Fluorescence spectra were recorded using a Cytation 3 Multi-Mode Reader and an Agilent Cary Eclipse fluorescence spectrophotometer. UV-vis spectra were recorded using an Agilent Cary 8454 UV-vis spectrophotometer. ^{1}H NMR and ^{13}C NMR spectra were recorded using a JEOL (400 MHz) NMR spectrometer. The peaks were internally referenced to TMS (0.00 ppm) or residual undeuterated solvent signal. The following abbreviations were used to explain multiplicities: s = singlet, d = doublet, t = triplet, q = quartet, m = multiplet, and dt = doublets of triplets, dd = doublets of doublets. High Resolution Mass Spectroscopy (HRMS) spectra was recorded on a Bruker impact II instrument (ESI-QToF). Liquid Chromatography Mass Spectroscopy (LC-MS) spectra were recorded on an Agilent 1260 Infinity II. Gas Chromatography (GC) spectra were recorded on an Agilent 7890A with a Flame Ionization Detector (FID).

For fluorescence measurement, solution of probes was prepared in ethanol. All of the metal ions were dissolved in distilled water form their perchlorate or nitrate salts where Hg^{2+} was prepared from its acetate salt. Anions were dissolved in distilled water from their sodium salts.

S.2. Synthesis and characterization of probes

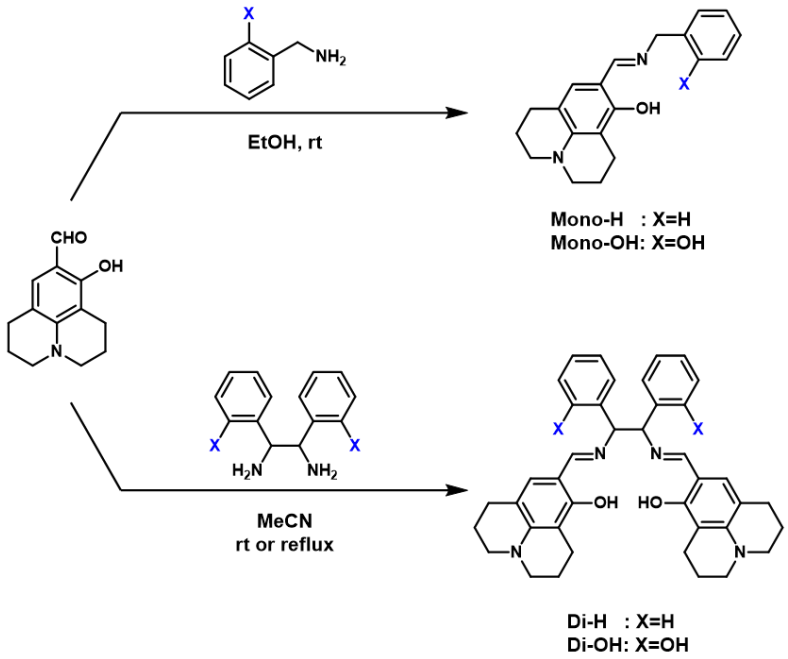

S.2.1. Synthesis of 9,9'-((1*E*,1'*E*)-((1,2-bis(2-hydroxyphenyl)ethane-1,2-diyl)bis(azaneylylidene))bis(methaneylylidene))bis(2,3,6,7-tetrahydro-1*H*,5*H*-pyrido[3,2,1-*ij*]quinolin-8-ol) (Di-OH)

To solution of 8-hydroxyjulolidine-9-carboxaldehyde (1.30 g, 6 mmole) in MeCN (40 mL), 2,2'-(1,2-diaminoethane-1,2-diyl)diphenol (3.0 mmole, 0.73 g) was added. The reaction mixture was refluxed for 48 h under Ar(g) and concentrated in *vacuo*. The obtained solid were washed with hot acetone and dried affording yellow solids (1.0 g, 1.56 mmole, 26%); ^{1}H-NMR (400 MHz, DMSO-d_6) δ 7.97 (s, 2H), 7.22 (d, J = 7.3 Hz, 2H), 6.92 (t, J = 7.0 Hz, 2H), 6.69 (d, J = 7.9 Hz, 2H), 6.63 (t, J = 7.3 Hz, 2H), 6.54 (s, 2H), 5.29 (s, 2H), 3.12 (s, 8H), 1.78 (d, J = 5.5 Hz, 8H); ^{1}H-NMR (400 MHz, DMF-d_7) δ 8.14 (s, 2H), 7.40 (d, J = 7.3 Hz, 2H), 6.95 (t, J = 7.6 Hz, 2H), 6.82 (d, J = 7.9 Hz, 2H), 6.67 (t, J = 7.3 Hz, 2H), 6.58 (s, 2H), 5.51 (s, 2H), 3.15 (t, J = 5.5 Hz, 8H), 2.57 (dt, J = 15.7, 6.6 Hz, 8H), 1.79-1.88 (m, 8H); ^{13}C-NMR (101 MHz, DMSO-d_6) δ 163.38, 160.02, 154.55, 145.90, 128.85, 128.63, 127.59, 126.91, 118.52, 115.12, 111.45, 107.25, 105.59, 68.65, 49.26, 48.91, 26.55, 21.55, 20.68, 20.13; ^{13}C-NMR (101 MHz, DMF-d_7) δ 164.39, 160.13, 155.47, 146.46, 129.46, 129.17, 127.99, 127.91, 119.04, 115.56, 112.19, 108.32, 106.38, 69.85, 49.97, 49.60, 27.23, 22.26, 21.39, 20.72; HRMS (ESI): m/z calcd for $C_{40}H_{43}N_4O_4^+$ $[M+H]^+$ 643.3279; found 643.3276.

S.2.2. Synthesis of 9,9'-((1*E*,1'*E*)-((1,2-diphenylethane-1,2-diyl)bis(azaneylylidene))bis(methaneylylidene))bis(2,3,6,7-tetrahydro-1*H*,5*H*-pyrido[3,2,1-*ij*]quinolin-8-ol) (Di-H).

To solution of 8-hydroxyjulolidine-9-carboxaldehyde (0.43 g, 2 mmole) in MeCN (30 mL), 1,2-diphenylethane-1,2-diamine (1.0 mmole, 0.21 g) was added. The reaction mixture was stirred at room temperature for 48 h under Ar(g) and concentrated in *vacuo*. After purification by column chromatography (silica, $CHCl_3$/MeOH, 40/1, v/v) **Di-H** were obtained as yellow solid (0.15 g, 0.25 mmole, 13%); ^{1}H-NMR (400 MHz, DMSO-d_6) δ 13.65 (s, 2H), 8.09 (s, 2H), 7.10-7.24 (m, 10H), 6.55 (s, 2H), 4.77 (s, 2H), 3.12 (t, J = 5.2 Hz, 8H), 2.50-2.56 (m, 8H), 1.79 (t, J = 5.5 Hz, 8H); ^{13}C-NMR (101 MHz, DMSO-d_6) δ 164.54, 157.92, 145.73, 141.01, 128.86, 127.91, 127.71, 126.79, 111.62, 107.17, 105.46, 77.74, 49.21, 48.83, 26.46, 21.41, 20.56, 20.03; HRMS (ESI): m/z calcd for $C_{40}H_{43}N_4O_2^+$ $[M+H]^+$ 611.3381; found 611.3371.

S.2.3. Synthesis of (*E*)-9-(((2-hydroxybenzyl)imino)methyl)-2,3,6,7-tetrahydro-1*H*,5*H*-pyrido[3,2,1-*ij*]quinolin-8-ol (Mono-OH).

To solution of 8-hydroxyjulolidine-9-carboxaldehyde (0.65 g, 3 mmole) in EtOH (30 mL), 2-(aminomethyl)phenol (0.37 g, 3 mmole) was added. The reaction mixture was stirred at room temperature for 48 h and the suspension was filtered. The filtered solid were washed with EtOH and dried affording greenish-yellow solids (0.80 g, 2.48 mmole, 83%); ^{1}H-NMR (400 MHz, DMSO-d_6) δ 13.87 (s, 1H), 9.56 (s, 1H), 8.17 (s, 1H), 7.07-7.13 (m, 2H), 6.75-6.83 (m, 2H), 6.66 (s, 1H), 4.57 (s, 2H), 3.12-3.17 (m, 4H), 2.57 (t, J = 6.1 Hz, 2H), 2.51 (d, J = 6.1 Hz, 2H), 1.81 (td, J = 11.4, 5.7 Hz, 4H); ^{13}C-NMR (101 MHz, DMSO-d_6) δ 163.95, 160.84, 154.98, 146.00, 128.83, 128.72, 128.08, 125.24, 118.85, 114.99, 111.48, 107.33, 105.74, 54.96, 49.28, 48.94, 26.63, 21.65, 20.71, 20.06; HRMS (ESI): m/z calcd for $C_{20}H_{23}N_2O_2^+$ $[M+H]^+$ 323.1754; found 323.1763.

S.2.4. Synthesis of (*E*)-9-((benzylimino)methyl)-2,3,6,7-tetrahydro-1*H*,5*H*-pyrido[3,2,1-*ij*]quinolin-8-ol (Mono-H).

To solution of 8-hydroxyjulolidine-9-carboxaldehyde (0.65 g, 3 mmole) in EtOH (30 mL), benzylamine (0.32 g, 3 mmole) was added. The reaction mixture was stirred at room temperature for 48 h and concentrated in *vacuo*. After purification by column chromatography (silica, $CHCl_3$/MeOH, 30/1, v/v) **Mono-H** were obtained as yellow oil (0.70 g, 2.28 mmole, 76%); ^{1}H-NMR (400 MHz, DMSO-d_6) δ 13.75 (s, 1H), 8.27 (s, 1H), 7.25-7.37 (m, 5H), 6.71 (s, 1H), 4.65 (s, 2H), 3.16 (dd, J = 11.6, 7.3 Hz, 4H), 2.59 (t, J = 6.4 Hz, 2H), 2.52 (t, J = 6.1 Hz, 2H), 1.82 (td, J = 11.6, 6.1 Hz, 4H); ^{13}C-NMR (101 MHz, DMSO-d_6) δ 164.74, 159.09, 145.81, 139.43, 128.79, 128.33, 127.36, 126.79, 111.63, 107.30, 105.61, 60.67, 49.24, 48.87, 26.56, 21.55, 20.62, 19.99; HRMS (ESI): m/z calcd for $C_{20}H_{23}N_2O^+$ $[M+H]^+$ 307.1805; found 307.1804.

S.3. UV-Vis Spectra

S.3.1. UV-Vis spectra of Di-OH, Di-H, Mono-OH and Mono-H

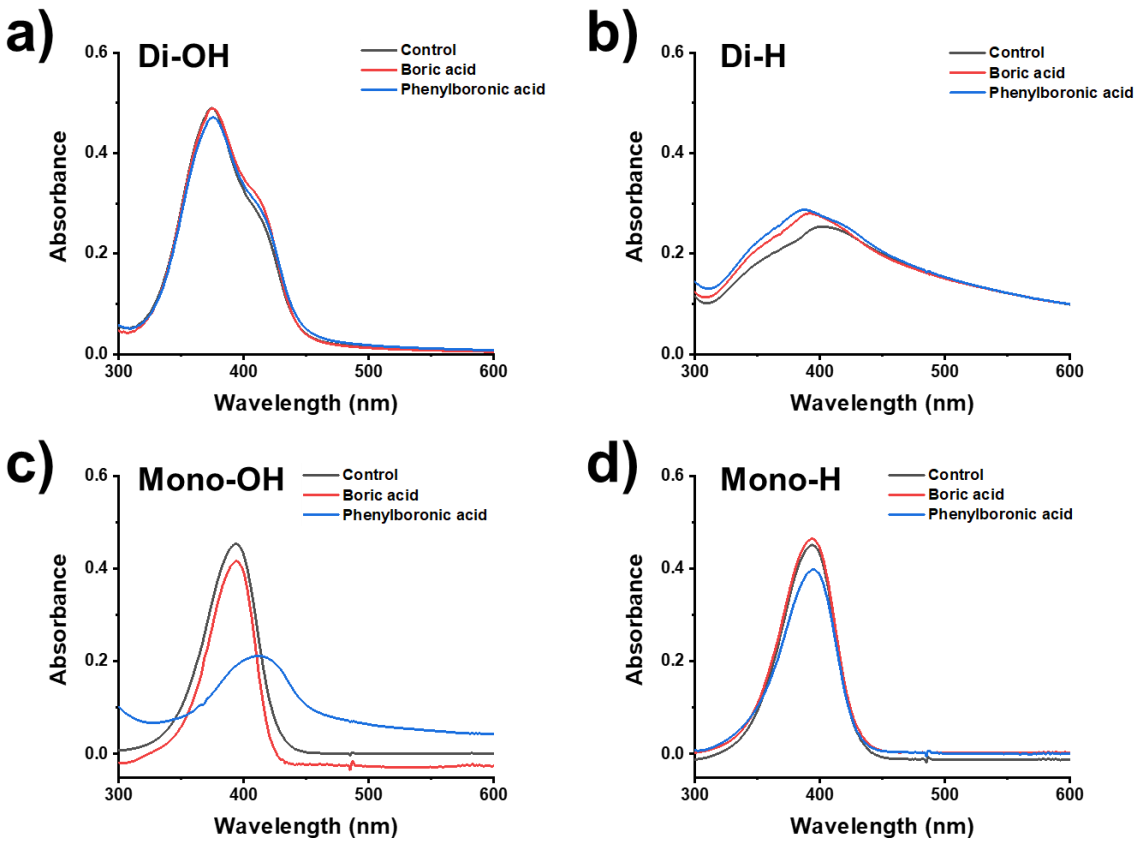

Fig. S1 UV-Vis absorption spectral change of 10 μM of a) **Di-OH**, b) **Di-H**, c) **Mono-OH** and d) **Mono-H** in the absence (black) and presence of boric acid (3 mM, red) or phenylboronic acid (3 mM, blue). MES buffer (50 mM, pH 6.0, EtOH : H_2O = 2 : 8). Absorbance spectra was measured 1 h after addition of boric acid or phenylboronic acid.

S.3.2. UV-Vis spectral change of Di-OH during the reaction with boric acid (BA)

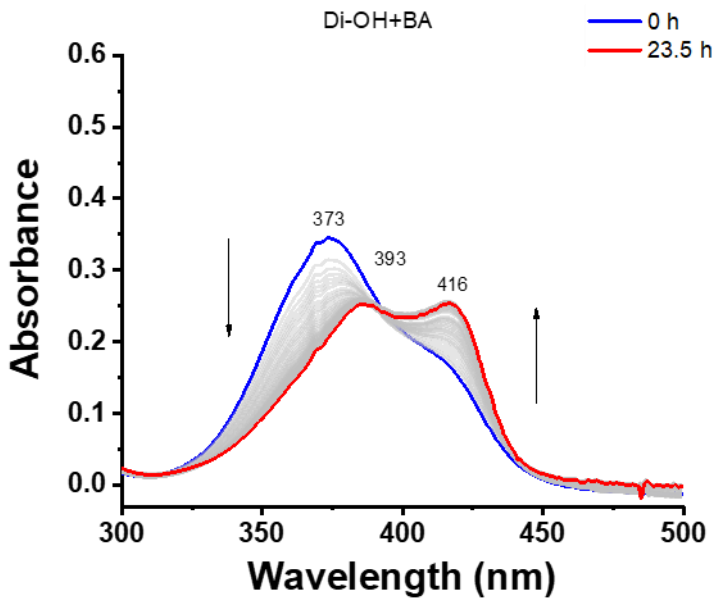

Fig. S2 UV-Vis spectral change of **Di-OH** (10 μM) in the presence of boric acid (3 mM) in MES buffer (50 mM, pH 6.0, EtOH:H_2O = 2:8).

S.4. Fluorescence Spectra

S.4.1. Fluorescence spectra of Di-OH, Di-H, Mono-OH and Mono-H

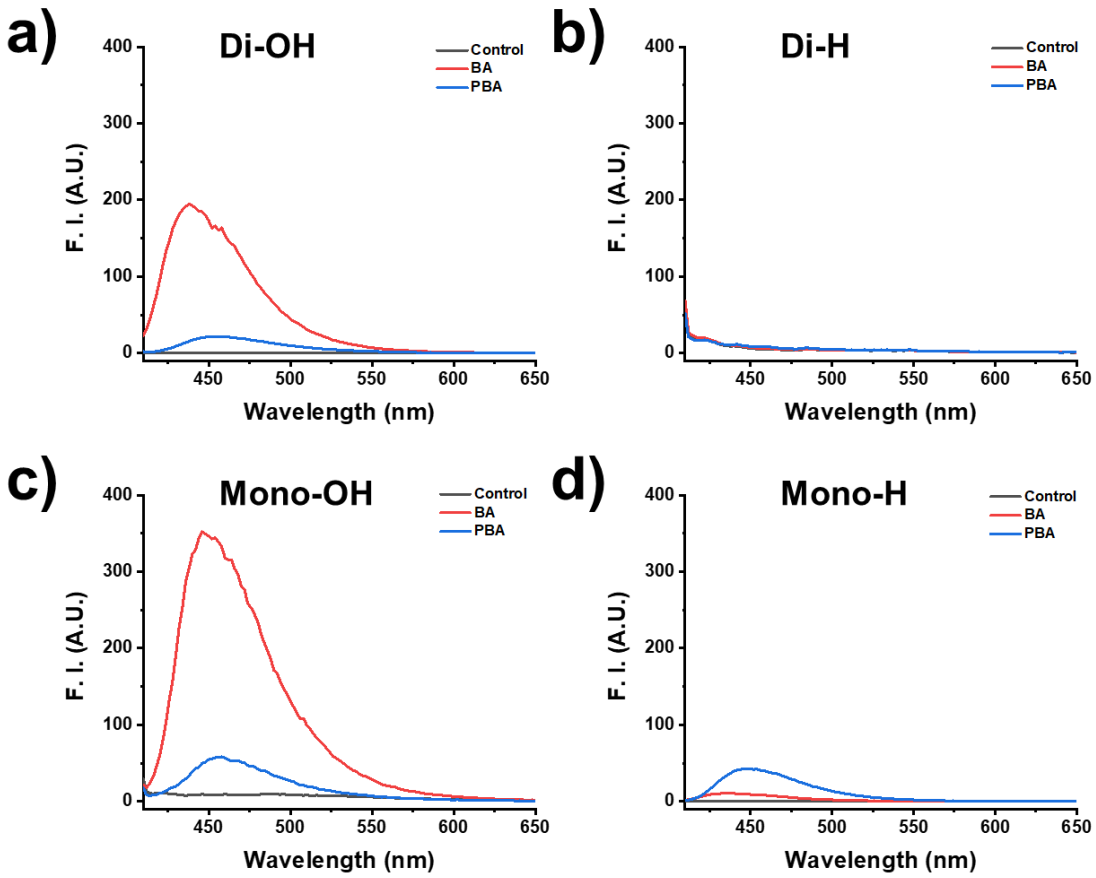

Fig. S3 Fluorescence spectral change of 10 μM of a) **Di-OH**, b) **Di-H**, c) **Mono-OH** and d) **Mono-H** in the absence (black) and presence of boric acid (3 mM, red) or phenylboronic acid (3 mM, blue). MES buffer (50 mM, pH 6.0, EtOH : H_2O = 2 : 8), λ_{ex} = 395 nm. Fluorescence spectra was measured 1 h after addition of boric acid or phenylboronic acid.

S.4.2. Fluorescence spectra of Di-OH in presence of BF_3-Et_2O

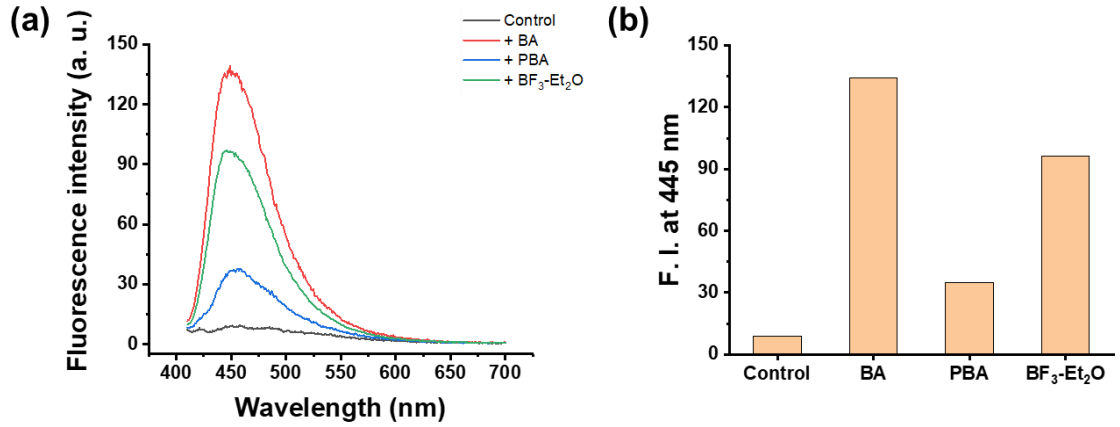

Fig. S4 (a) Fluorescence spectra of **Di-OH** in the absence (black) and presence of BA (red), PBA (blue), and BF_3-Et_2O (green), (b) Plot of fluorescence intensity at 445 nm. [**Di-OH**] = 10 μM, [BA]=[PBA]=[BF_3-Et_2O]= 3 mM, reaction time: 1h, pH 6.0 MES (50 mM, EtOH:H_2O = 2:8).

S.5. Fluorescence quantum yield of probes in the presence of boric acid (BA) or phenylboronic acid (PBA)

To calculate the relative fluorescence quantum yield, coumarin 153 (Φst = 0.53) in EtOH was used as the standard dye.[S1] The slope of each compound was calculated by plotting the absorbance on the x-axis and the fluorescence intensity at 445 nm on the y-axis. The quantum yield (Φ) was calculated using the following equation.

$$\Phi = \Phi st \times \frac{Compound\ \ slope}{Standard\ \ slope} \times \frac{Compound\ \ solvent\ \ refractive\ \ index^2}{Standard\ \ solvent\ \ refractive\ \ index^2}$$

Table S1 Quantum yield (Φ) of **Di-OH**, **Mono-OH**, **Di-H** and **Mono-H** in the presence of boric acid (BA) or phenylboronic acid (PBA).

Probe	Control	BA[a]	PBA[a]
Di-OH	0.00119	0.02571 (X 21.67)	0.00609 (X 5.13)
Mono-OH	0.00493	0.44342 (X 89.86)	0.27449 (X 55.63)
Di-H	0.00596	0.00157 (X 0.26)	0.00207 (X 0.35)
Mono-H	0.00038	0.00948 (X 24.94)	0.05806 (X 152.68)

[a] Reaction time: 1h

S.6. Fluorescence response of Di-OH and Mono-OH to boric acid (BA) and mixture of BA and phenylboronic acid (PBA)

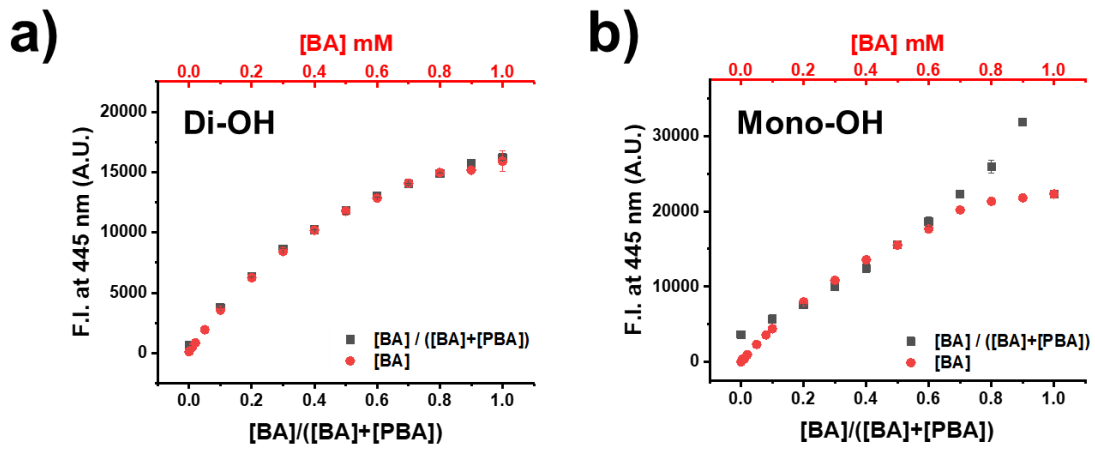

Fig. S5 Fluorescence intensities of 10 μM of a) **Di-OH** and b) **Mono-OH** upon addition various concentrations of BA (red) and mixtures of BA and PBA (black). MES buffer (50 mM, pH 6.0, EtOH : H_2O = 2 : 8), λ_{ex} = 395 nm.

S.7. pH Screening

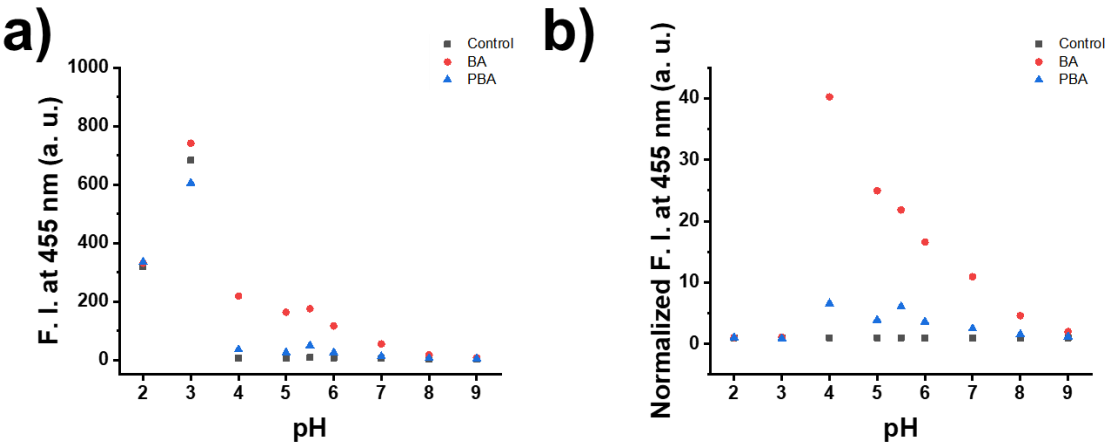

Fig. S6 (a) Fluorescence intensity of **Di-OH** (10 μM) at 455 nm in the presence of boric acid (3 mM) or phenylboronic acid (3 mM) in various buffer conditions. (b) Normalized fluorescence intensity at 455nm. (pH 2-3 Britton-Robinson buffer, pH 4-5 acetate, pH 5.5-6 MES, pH 7-9 Tris; 50 mM, EtOH:H_2O = 2:8), λ_{ex} = 395 nm. Fluorescence spectra was measured 1 h after addition of boric acid or phenylboronic acid

S.8. Solvent Screening

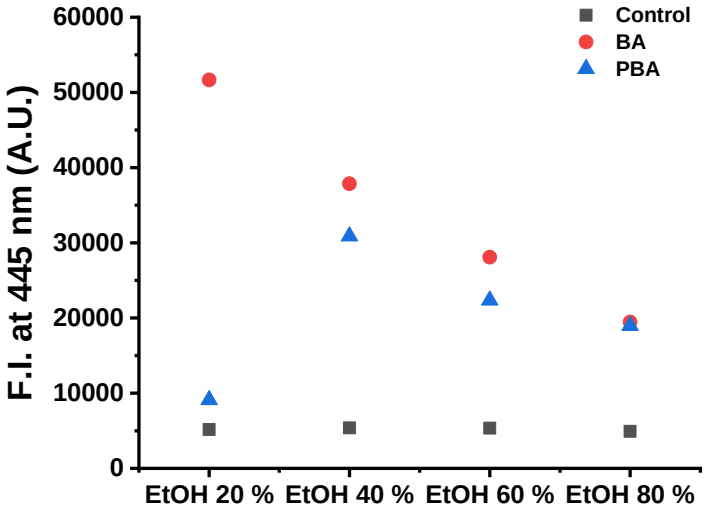

Fig. S7 Fluorescence intensity at 445 nm of **Di-OH** (10 μM) in the absence (black) and presence of boric acid (3 mM, red) or phenylboronic acid (3 mM, blue) under various concentrations of EtOH. MES buffer (50 mM, pH 6.0), λ_{ex} = 395 nm.

S.9. Calculation of limit of detection (LOD) for boric acid

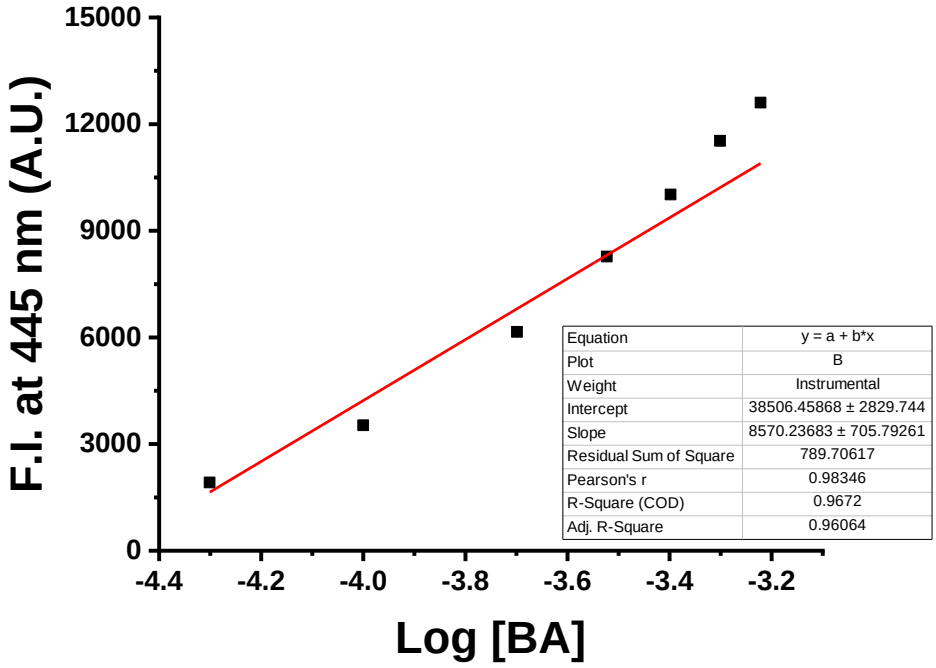

Fig. S8 Limit of detection of boric acid (BA). **Di-OH** (10 μM) with various concentrations (0.05–0.6 mM) of boric acid in MES buffer (50 mM, pH 6.0, EtOH:H_2O = 2:8), λ_{ex} = 395 nm.

The limit of detection (LOD) for boric acid was obtained from the low concentration range of boric acid (0.05–0.6 mM) in the boric acid titration (see Fig. 1(b)). A linear function was obtained when log[BA] was plotted against fluorescence intensity at 445 nm. The LOD was estimated form the x-intercept of this function.

Intercept = 38506.45868

Slope = 8570.23683

R^2 = 0.967

LOD = 32 μM

S.10. Selectivity and competitivity

S.10.1. Selectivity and competitivity under various cations without masking reagents

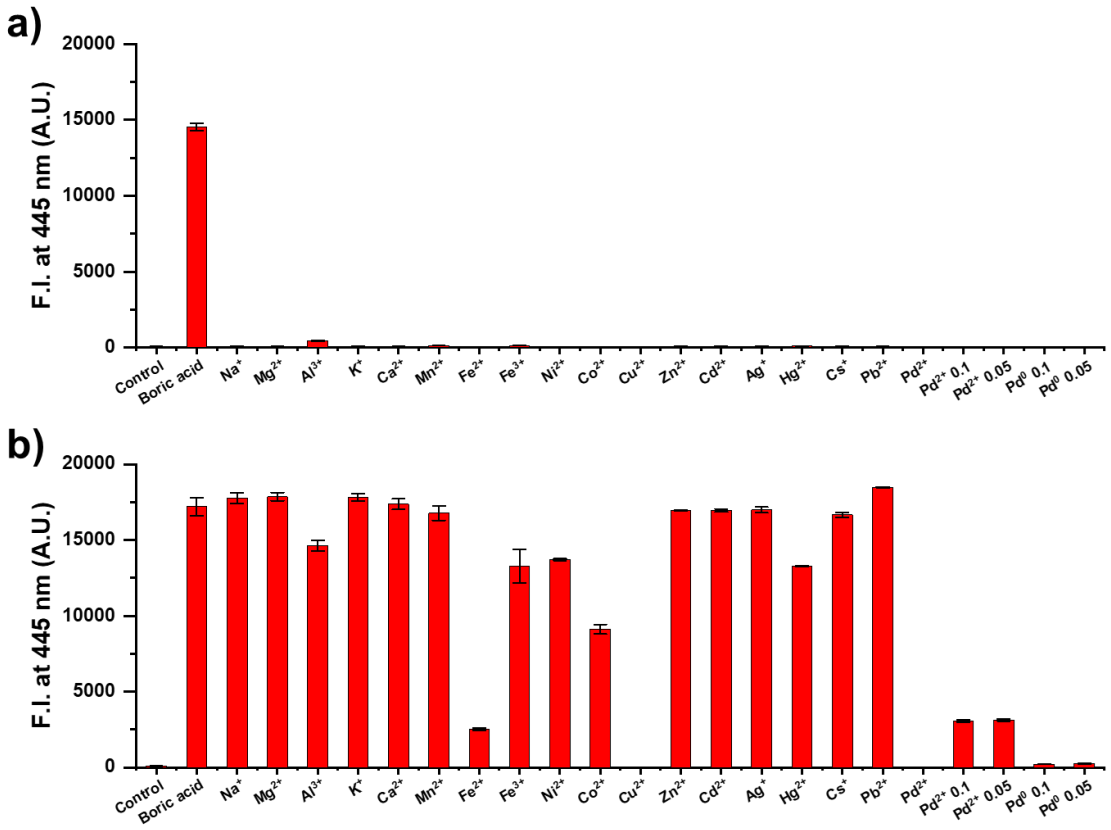

Fig. S9 Fluorescence intensity at 445 nm of **Di-OH** (10 μM) a) in presence of various cations (150 equiv.) and b) mixture of BA (150 equiv.) + analyte (150 equiv.) in MES buffer (50 mM, pH 6.0, EtOH : H_2O = 2 : 8), λ_{ex} = 395 nm.

S.10.2. Masking of palladium using masking reagents

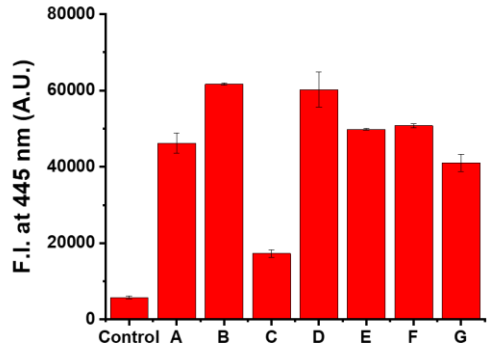

	Masking Reagent	Recovery (%)
Control	-	9.0
A	Sodium thiosulfate	72.0
B	Cysteamine·HCl	**96.0**
C	Ammonium thiocyanate	26.9
D	Cysteamine	**93.8**
E	Thiourea	77.6
F	Imidazolidinethione	79.1
G	Sodium sulfide	63.9

Fig. S10 Fluorescence intensity at 445 nm of **Di-OH** (10 μM) in presence boric acid (150 equiv.), Pd $(OAc)_2$ (50 μM) and various masking reagents (200 equiv.) in MES buffer (50 mM, pH 6.0, EtOH : H_2O = 2 : 8), λ_{ex} = 395 nm.

S.11. Binding study between Di-OH and boric acid

S.11.1. ^{1}H-NMR based binding study

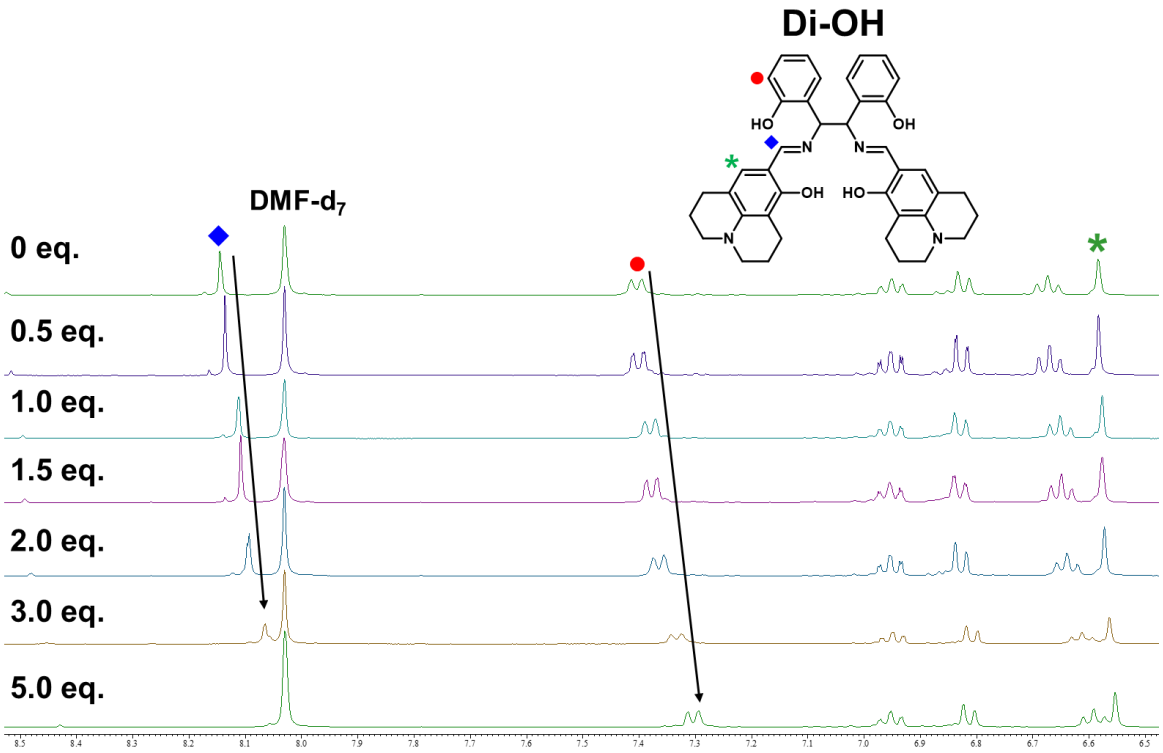

Fig. S11 ^{1}H-NMR spectra (DMF-d_7) of **Di-OH** (5 mM) after adding various concentrations of boric acid.

S.11.2. Fluorescence-based Job plot analysis

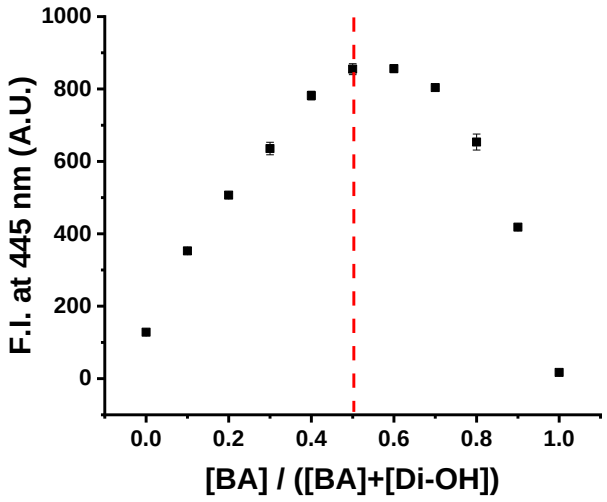

Fig. S12 Fluorescence intensity at 445 nm with varying boric acid (BA) concentrations. [BA] + [**Di-OH**] = 50 μM in MES buffer (50 mM, pH 6.0, EtOH : H_2O = 2 : 8), λ_{ex} = 395 nm.

S.11.3. Mass-based binding assay

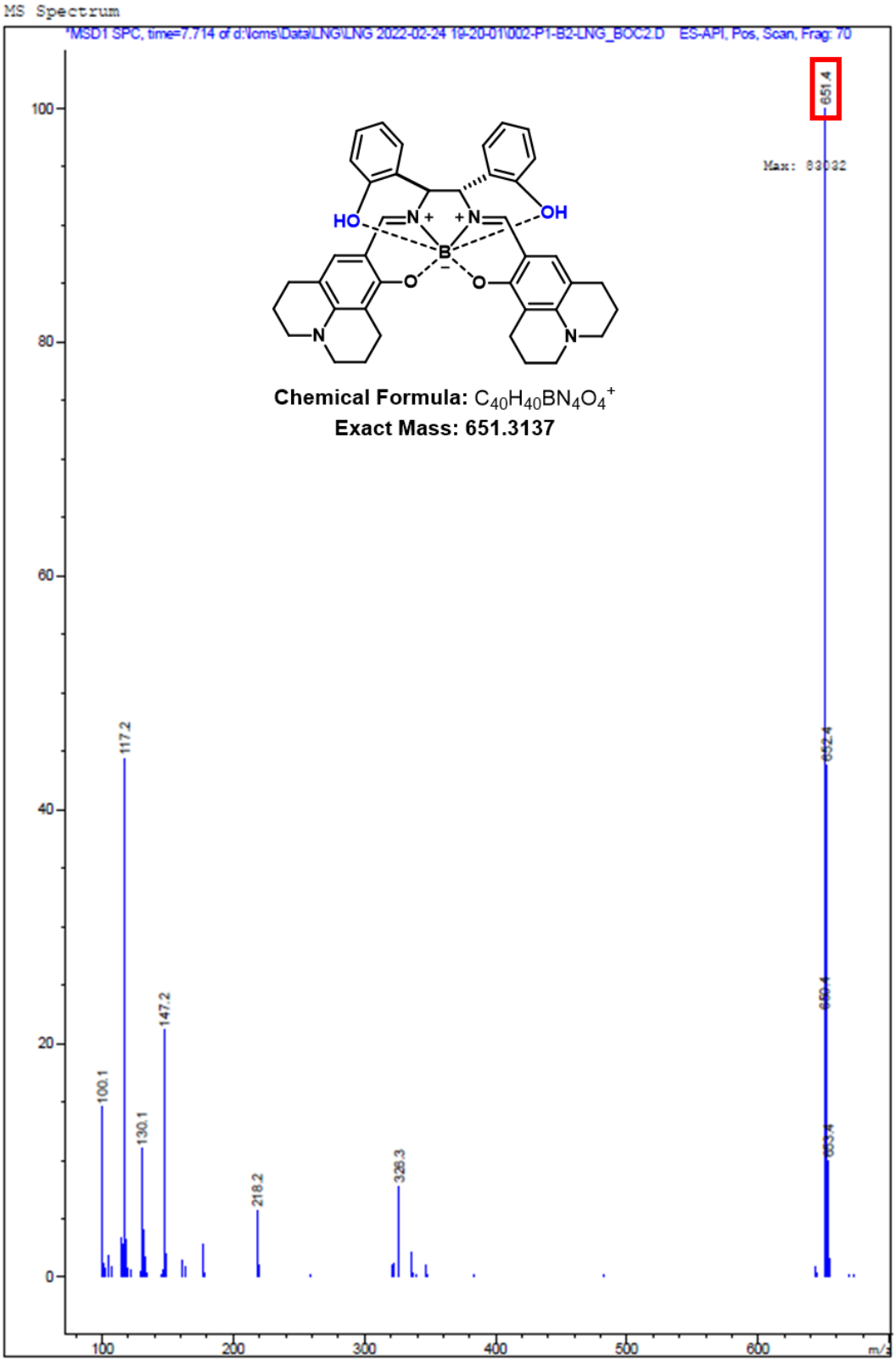

Fig. S13 LC-MS spectrum of **Di-OH**-boric acid adduct.

S.11.4. Probable sensing mechanism of boric acid (BA)

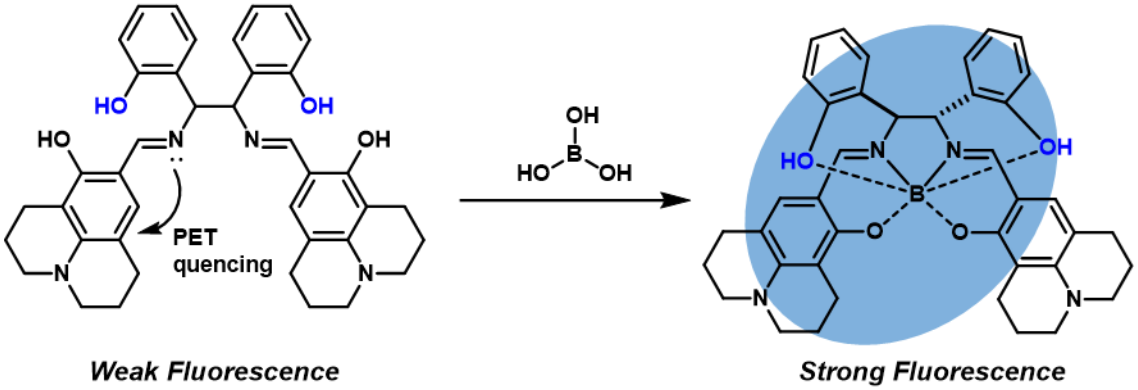

Scheme S1. Plausible sensing mechanism of BA based on **Di-OH**.

S.12. Application of Di-OH to screening the conversion of Suzuki-Miyaura cross coupling reactions

S.12.1. Screening of boronic acids used in Suzuki-Miyaura coupling reaction

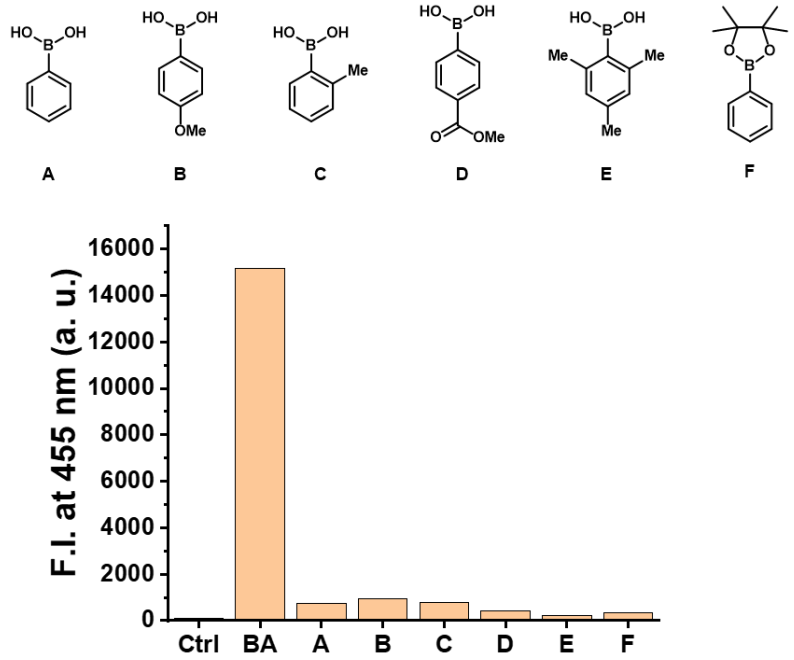

Fig. S14 Fluorescence intensity at 445 nm of **Di-OH** (10 μM) in presence of various analytes (3 mM) in MES buffer (50 mM, pH 6.0, EtOH:H_2O = 2:8). λ_{ex} = 395 nm. (ctrl: control, BA: boric acid, A: phenylboronic acid, B: (4-methoxyphenyl)boronic acid, C: (2-methylphenyl)boronic acid, D: (4-(methoxycarbonyl)phenyl)boronic acid, E: (2,4,6-trimethylphenyl) boronic acid, F: phenylboronic acid pinacol ester).

S.12.2. Experimental procedure for the Suzuki-Miyaura coupling reactions

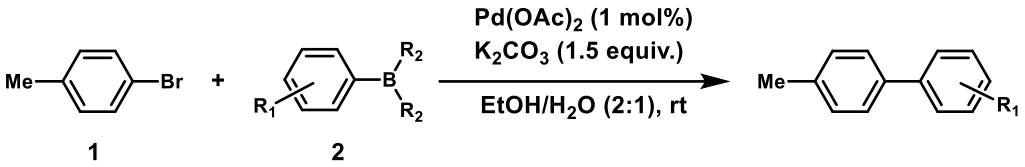

1 2

To a 5 mL vial containing a PTFE-coated magnetic stirring bar, $Pd(OAc)_2$ (0.003 mmol), and 1.5 mL of mixed EtOH/H_2O (2:1) solvent was added. To this solution, 4-bromotoluene (0.3 mmol), boronic acid derivatives (0.3 mmol), and K_2CO_3 (0.45 mmol) were added. The reaction mixture was stirred vigorously at room temperature for 2h. The reaction was monitored by thin layer chromatography (TLC). After the starting material was consumed, the reaction mixture was diluted with ethyl acetate and H_2O.

S.12.3. Experimental procedure for the Suzuki-Miyaura cross coupling analyses with fluorescence spectroscopy and gas-chromatography

To analyze yield and conversion for Suzuki-Miyaura coupling reaction, a standard curve was prepared using GC and its correlation with fluorescence-based calculation of conversion was compared. For GC analysis, octadecane was used as a standard material. After the reaction, the reaction mixture was diluted with ethyl acetate and H_2O. For analysis of boronic acid derivatives, 1ml of propane-1,3-diol (0.75 mmol) was added to the 2-fold diluted organic layer. The organic layer was further diluted 100-fold, and analyzed by GC. For analysis of boric acid, the 2-fold aqueous layer was further diluted 60-fold. Then, 20 μL of this solution was added to 180 uL of buffered solution (50 mM, pH 6.0 MES buffer, EtOH : H_2O = 2:8) containing **Di-OH** (10 μM). Fluorescence intensity was measured using a plate reader. The fluorescence value was converted to the fluorescence conversion using a standard curve.

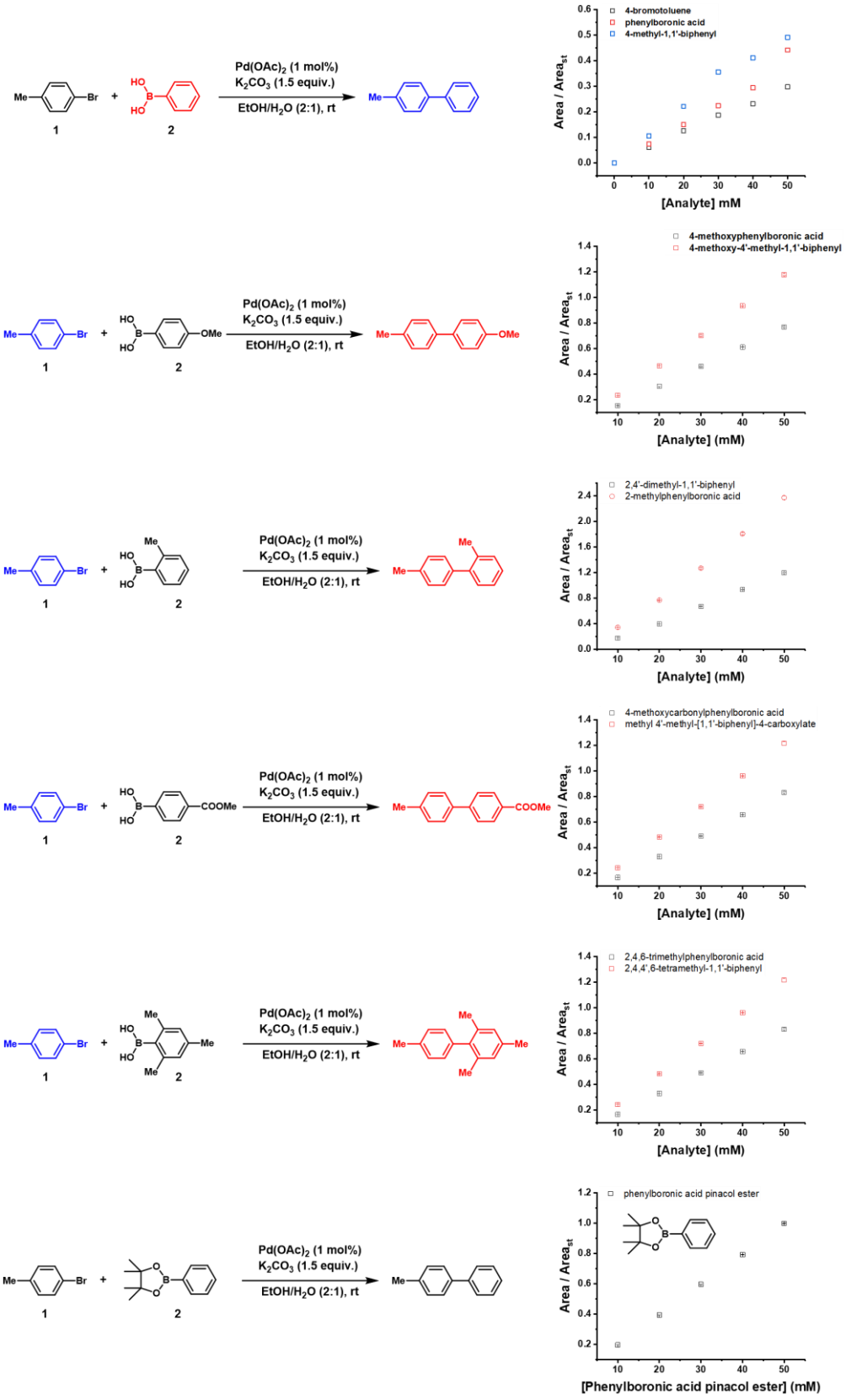

Fig. S15 GC standard curve of substrates and products used for Suzuki-Miyaura coupling reaction.

Catalytic reaction screening - Cal. Yield

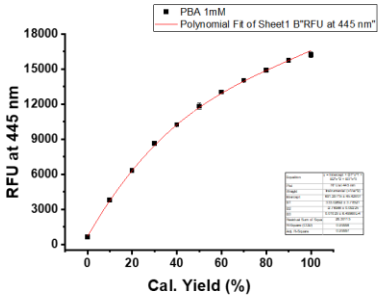

		Value	Standard Error	t-Value	Prob>|t|
RFU at 445 nm	Intercept	691.29715	45.42807	15.2174	1.27392E-6
	B1	333.02692	3.78521	87.98101	6.45404E-12
	B2	-2.76946	0.09225	-30.02217	1.17281E-8
	B3	0.01029	6.49968E-4	15.83513	9.70985E-7

Standard Error was scaled with square root of reduced Chi-Sqr.

Statistics

	RFU at 445 nm
Number of Points	11
Degrees of Freedom	7
Residual Sum of Squares	26.30115
R-Square (COD)	0.99998
Adj. R-Square	0.99997

1 mM = 100 %

105

Fig. S16 Fluorescence-based standard curve.

S.13. Spectra

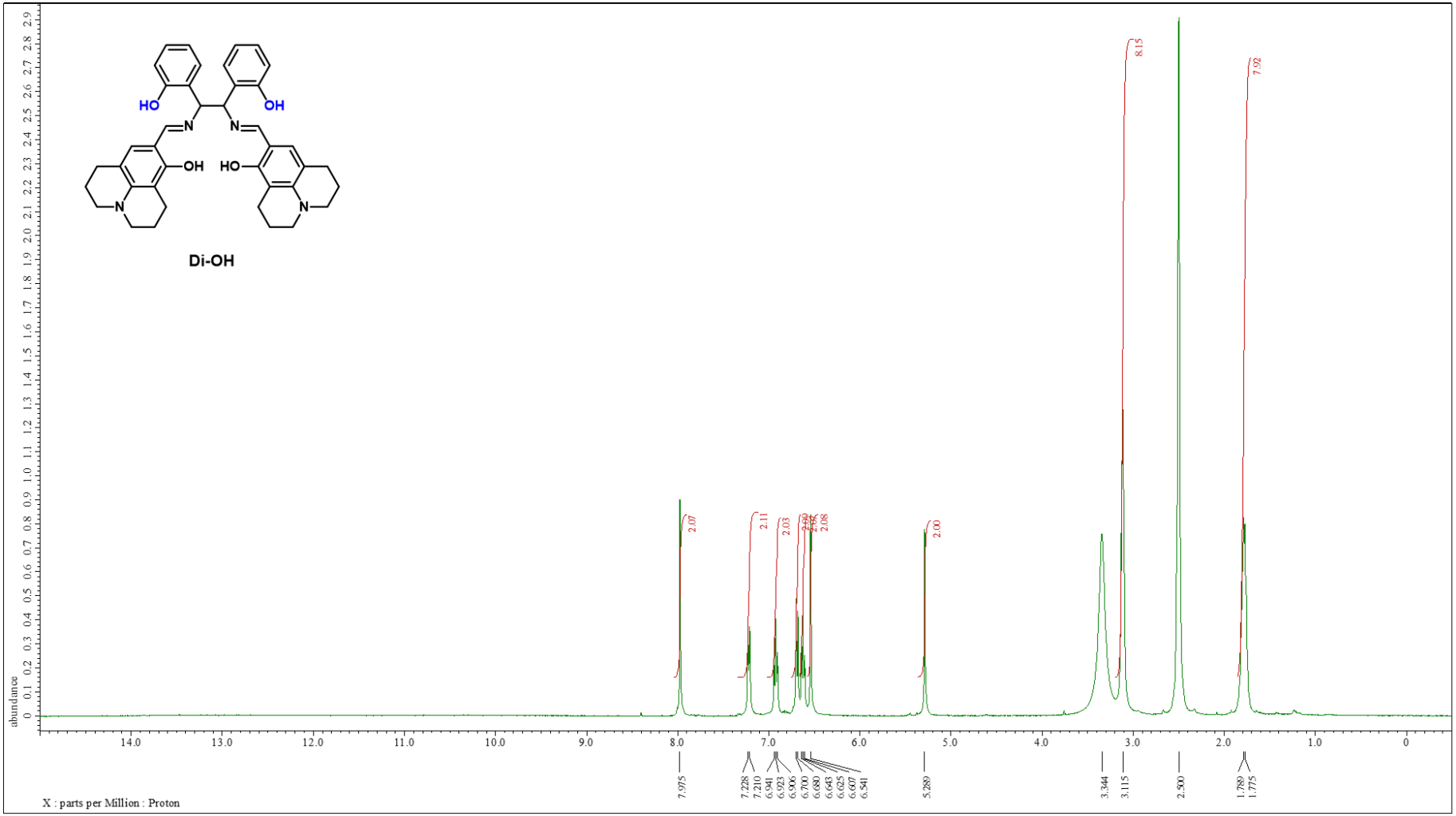

Fig. S17 ^{1}H NMR spectrum of **Di-OH** in DMSO-d_6.

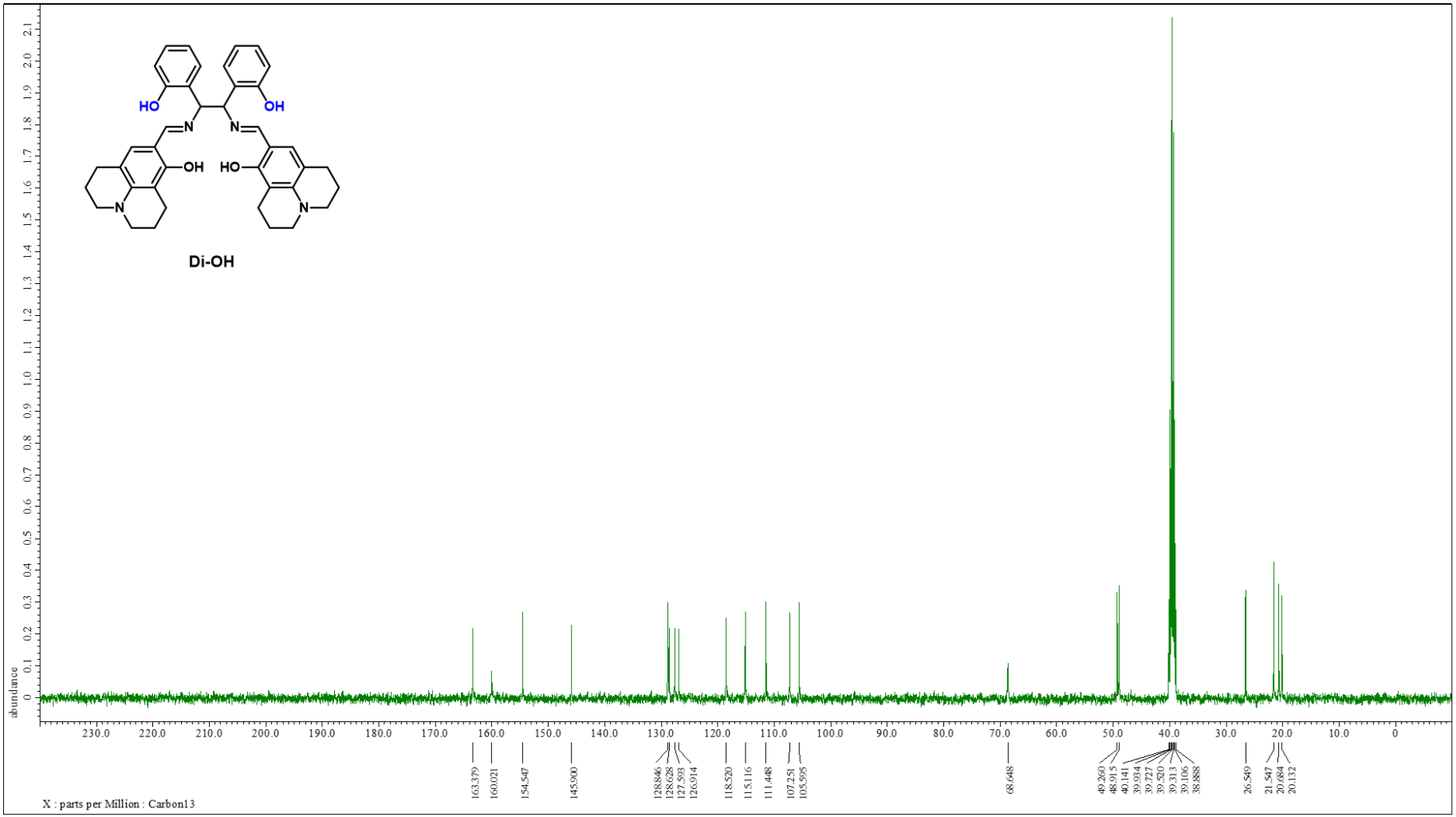

Fig. S18 ^{13}C NMR spectrum of **Di-OH** in DMSO-d_6.

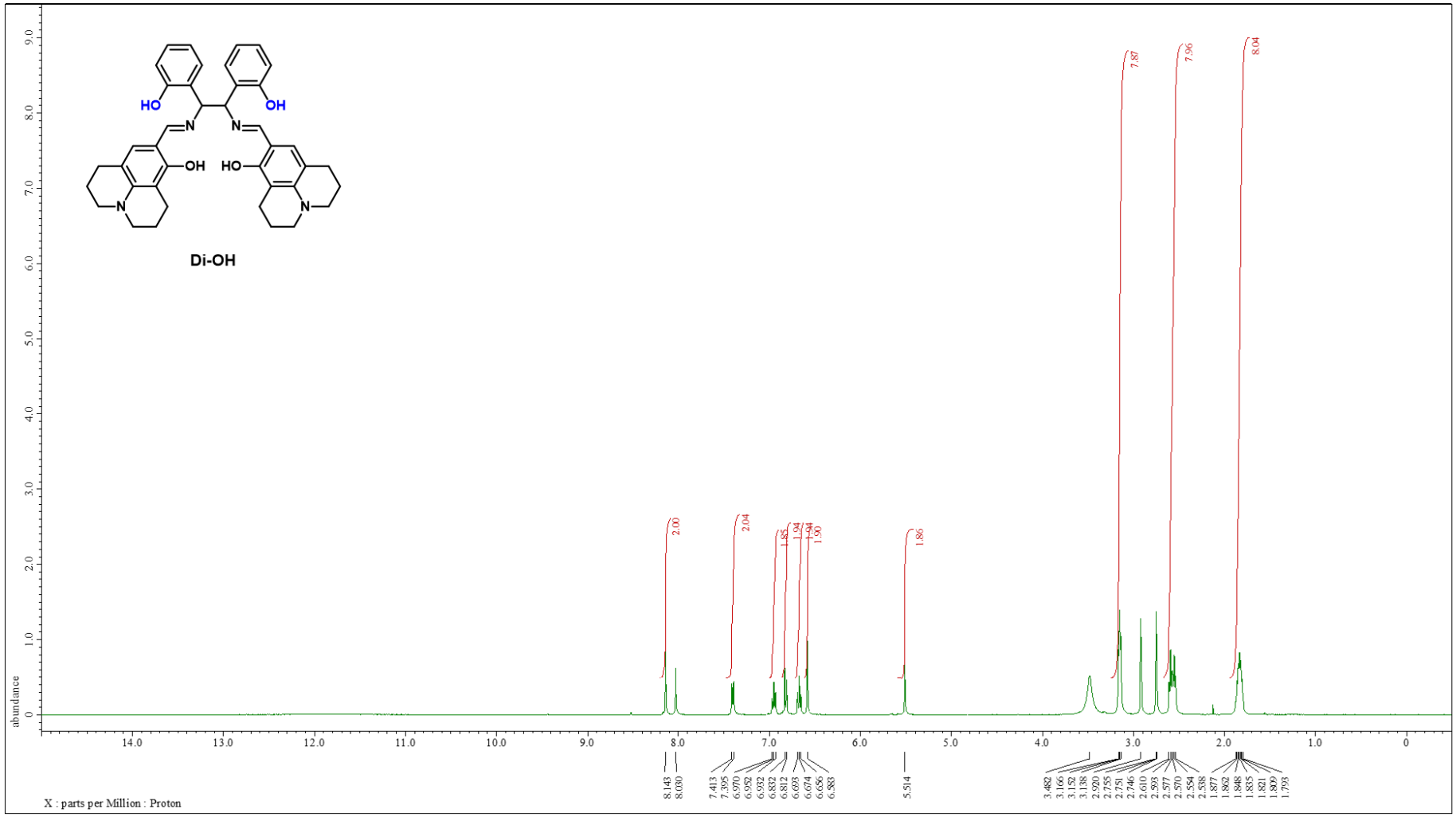

Fig. S19 ^{1}H NMR spectrum of **Di-OH** in DMF-d_7.

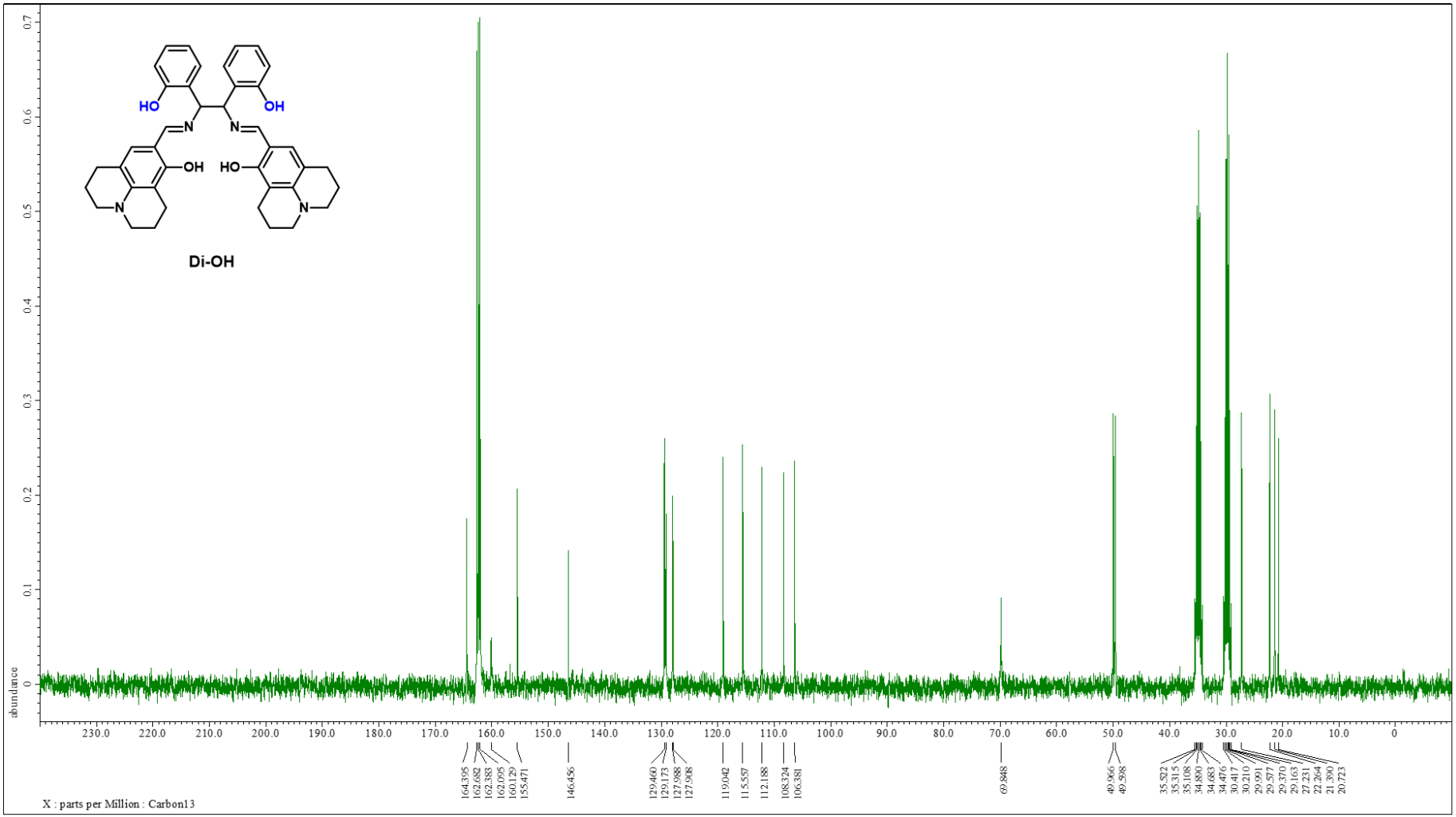

Fig. S20 ^{13}C NMR spectrum of **Di-OH** in DMF-d_7.

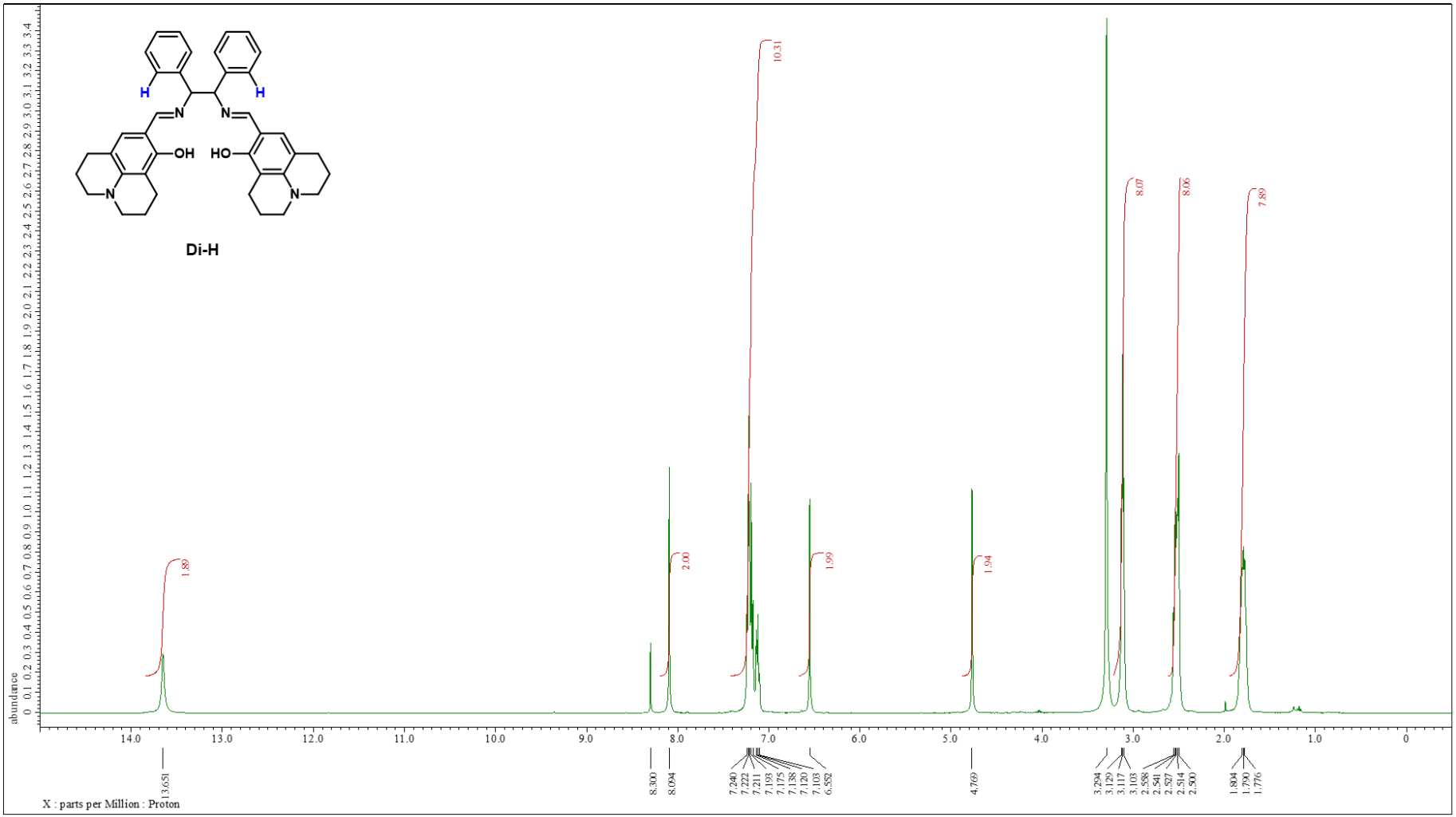

Fig. S21 ^{1}H NMR spectrum of **Di-H** in DMSO-d_6.

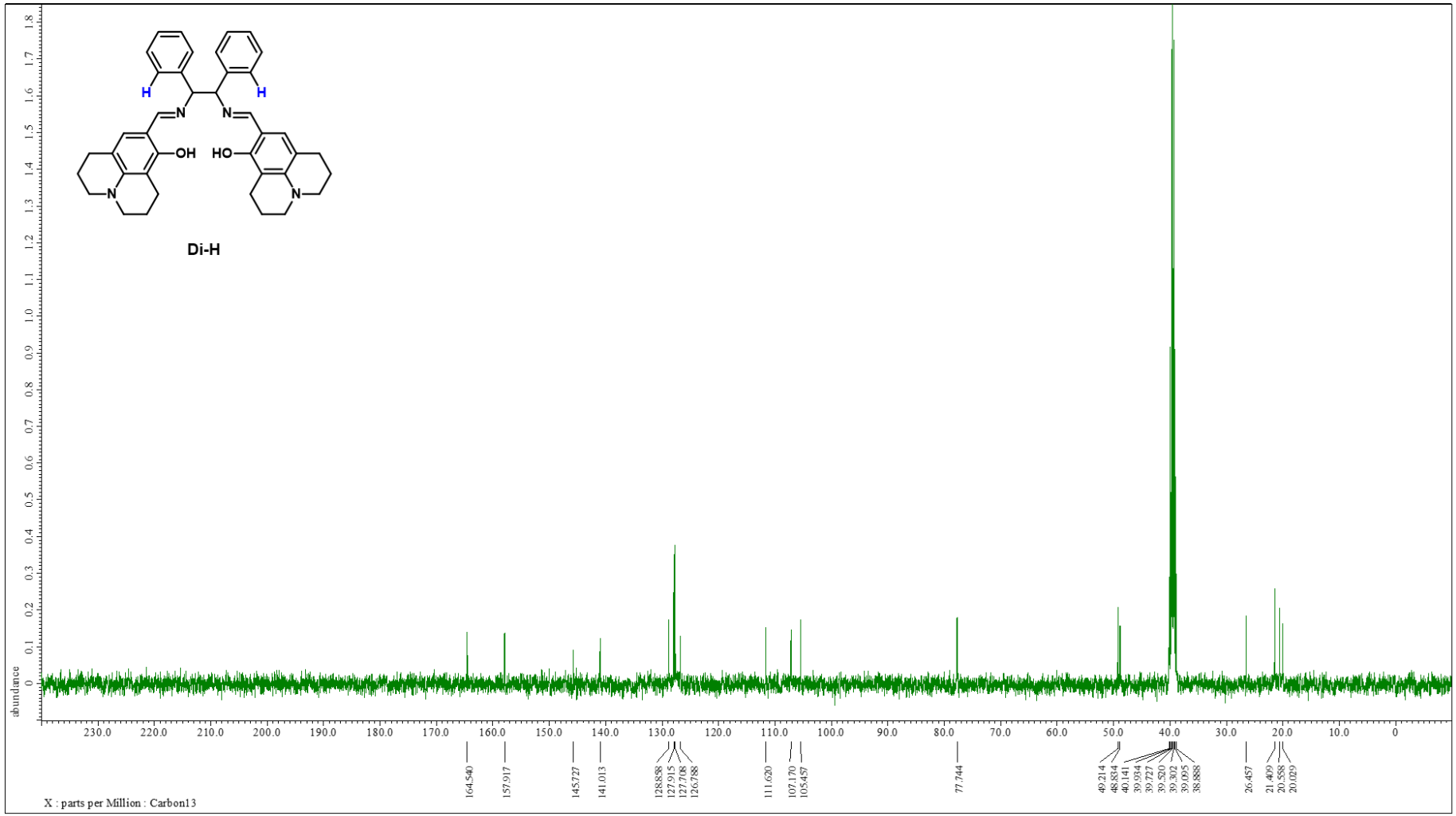

Fig. S22 ^{13}C NMR spectrum of **Di-H** in DMSO-d_6.

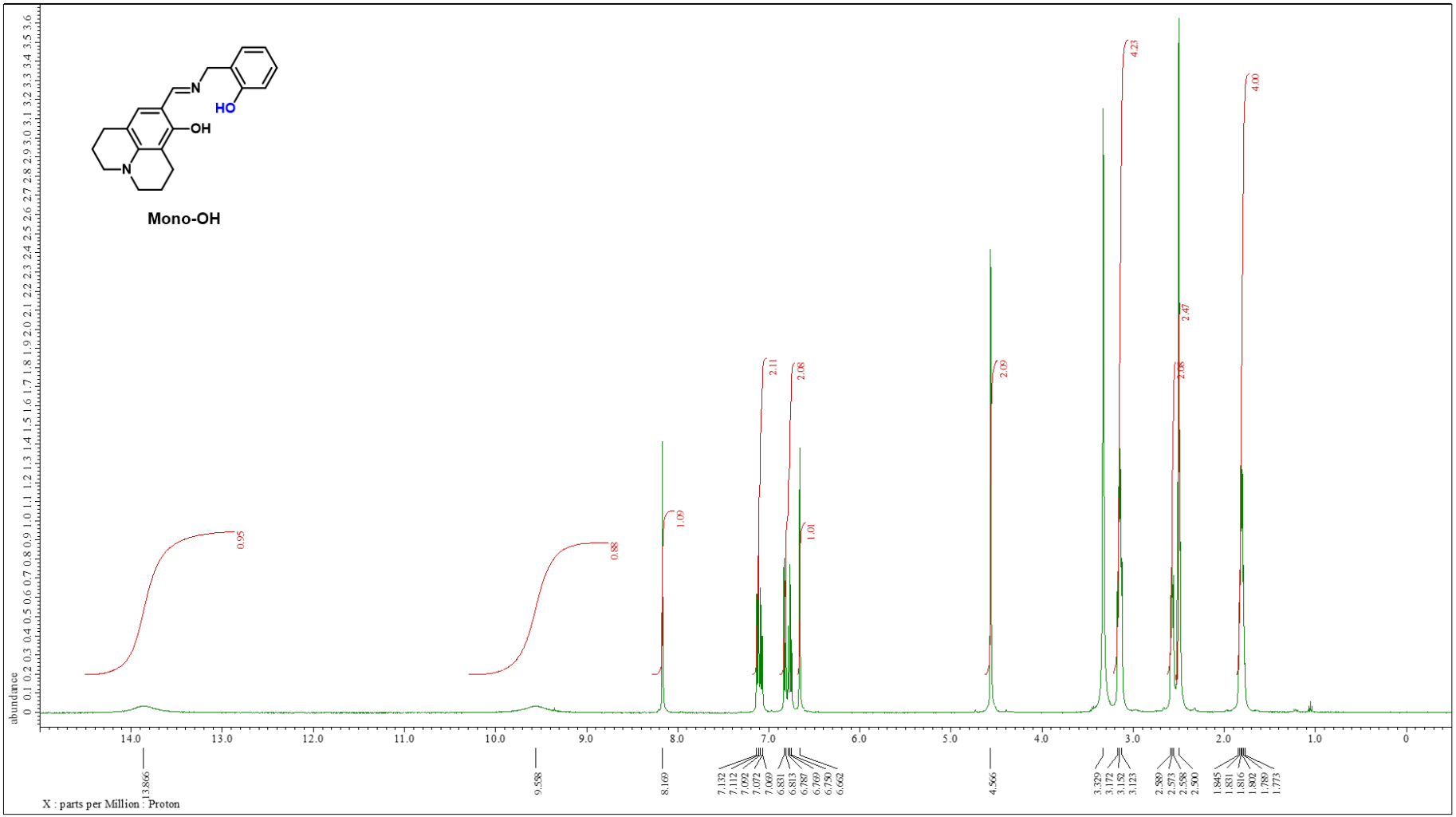

Fig. S23 ^{1}H NMR spectrum of **Mono-OH** in DMSO-d_6.

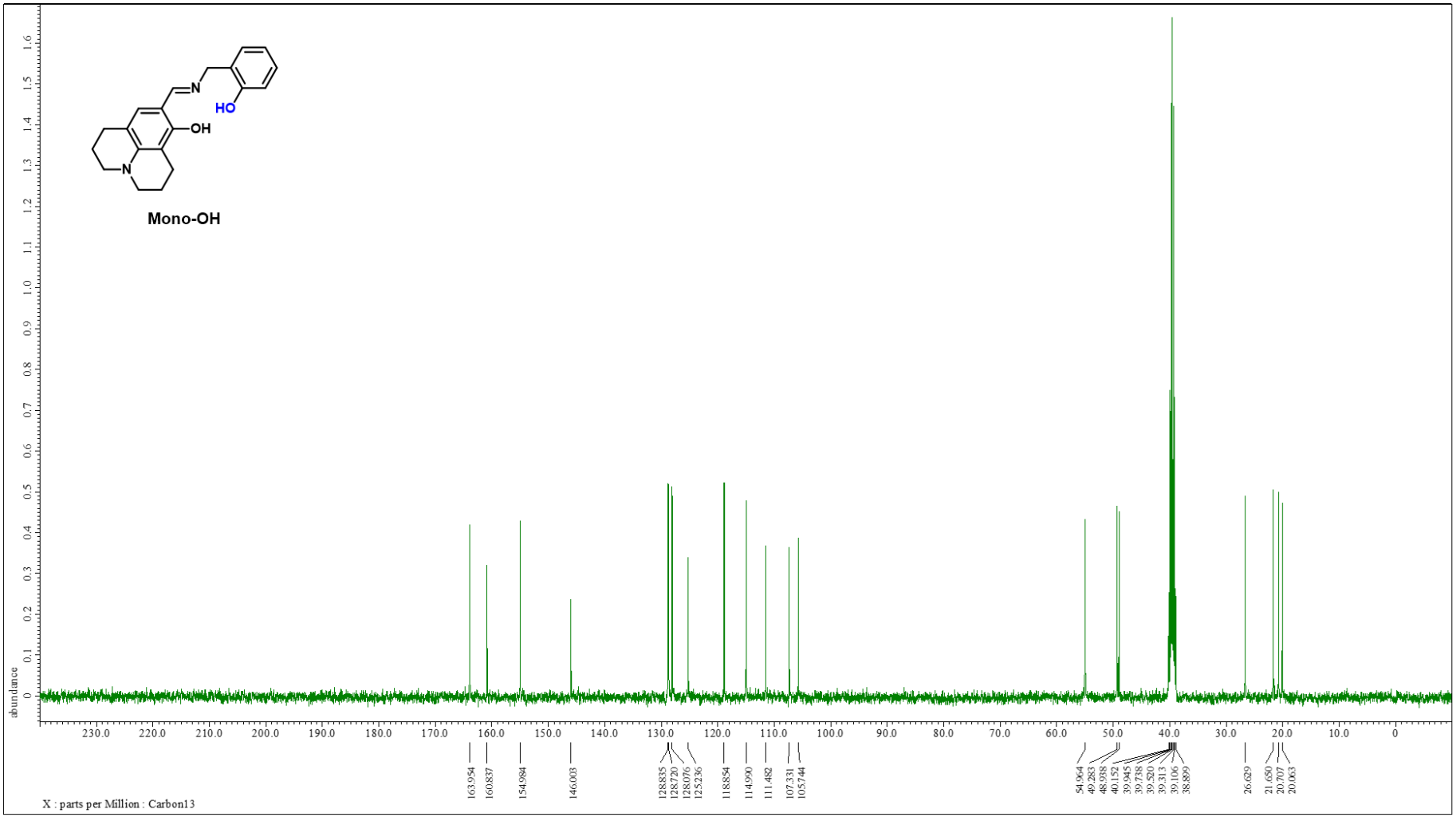

Fig. S24 ^{13}C NMR spectrum of **Mono-OH** in DMSO-d_6.

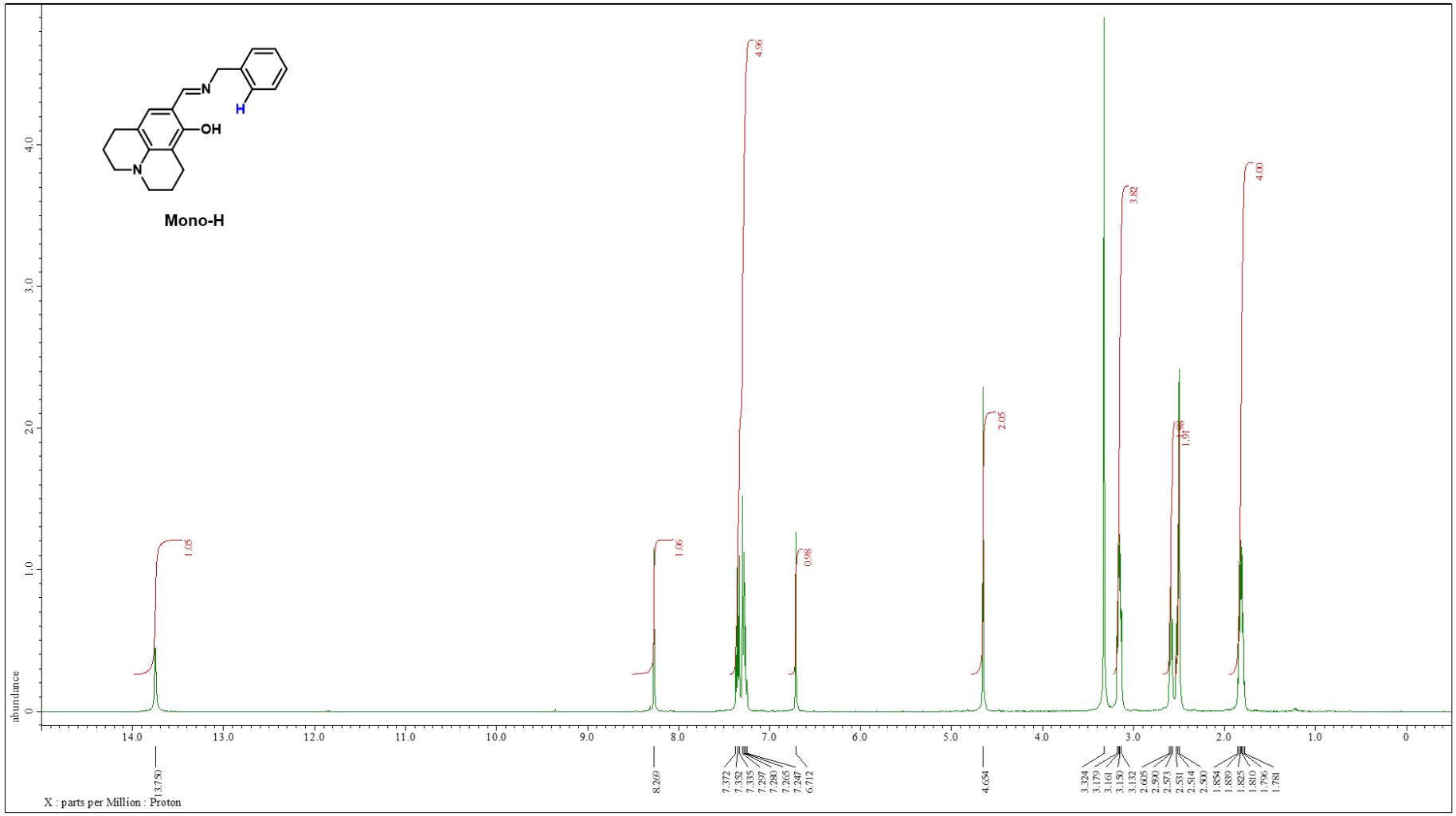

Fig. S25 ^{1}H NMR spectrum of **Mono-H** in DMSO-d_6.

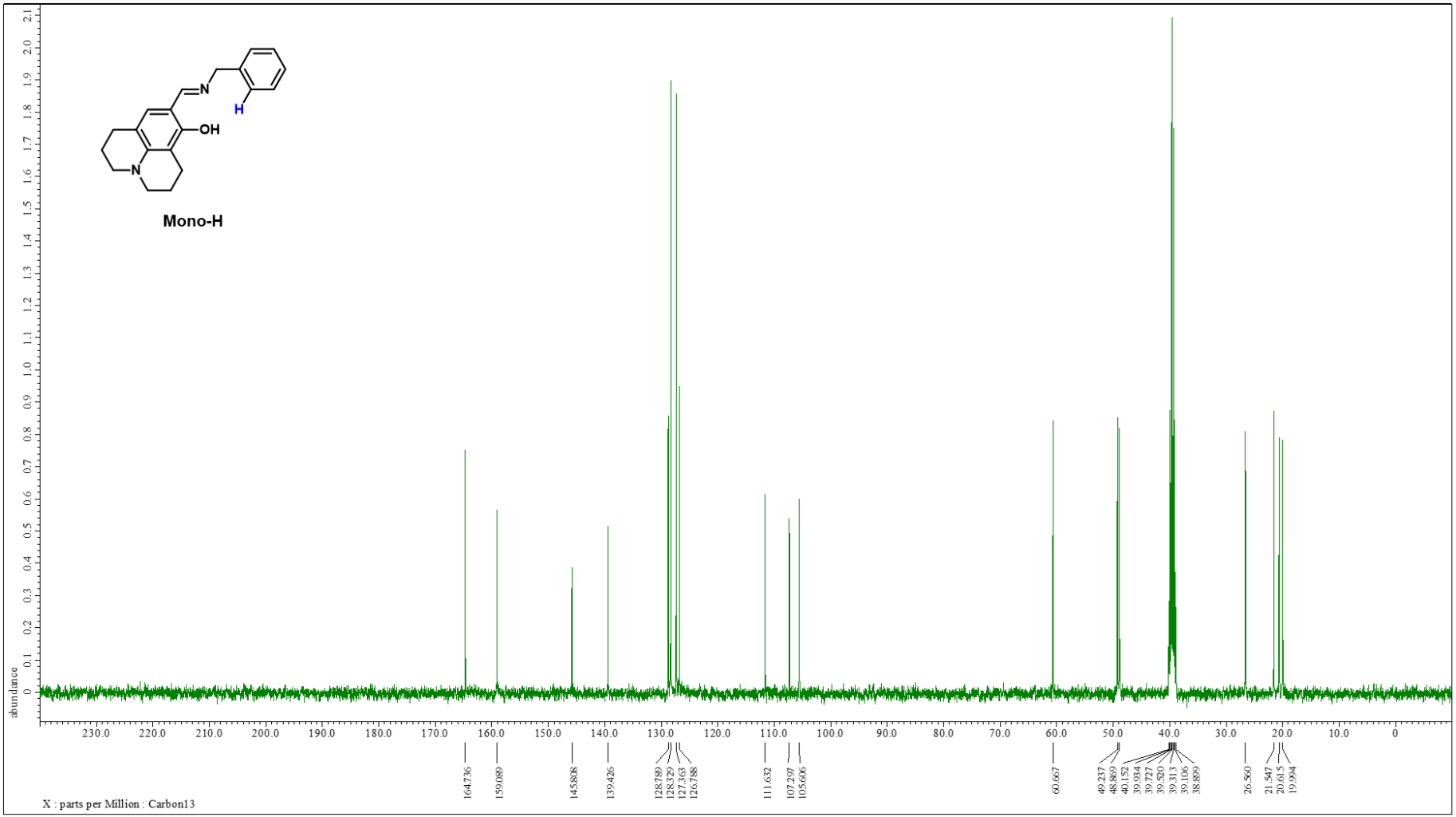

Fig. S26 ^{13}C NMR spectrum of **Mono-H** in DMSO-d_6.

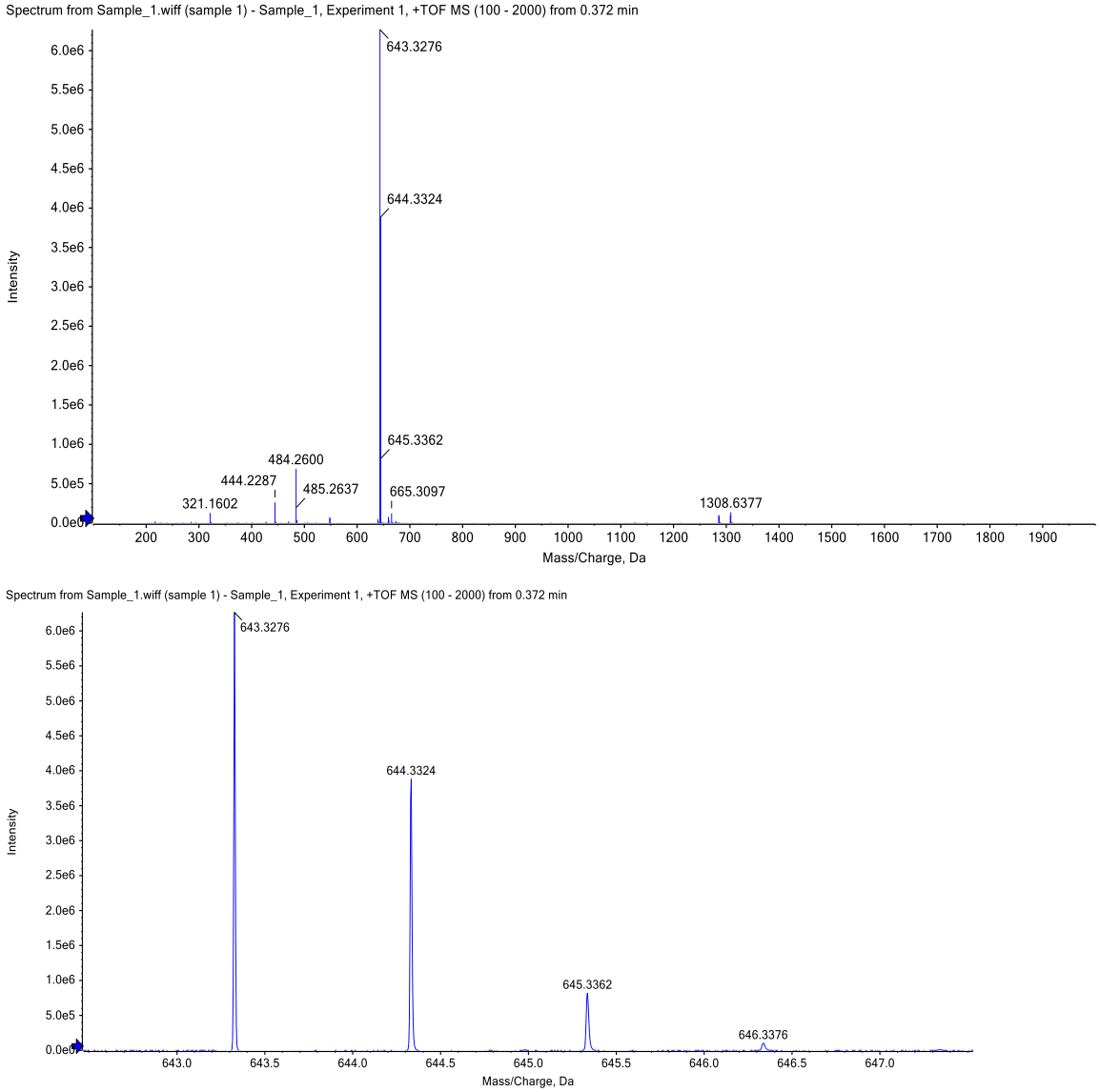

Fig. S27 HRMS spectrum and isotope distribution pattern of **Di-OH**.

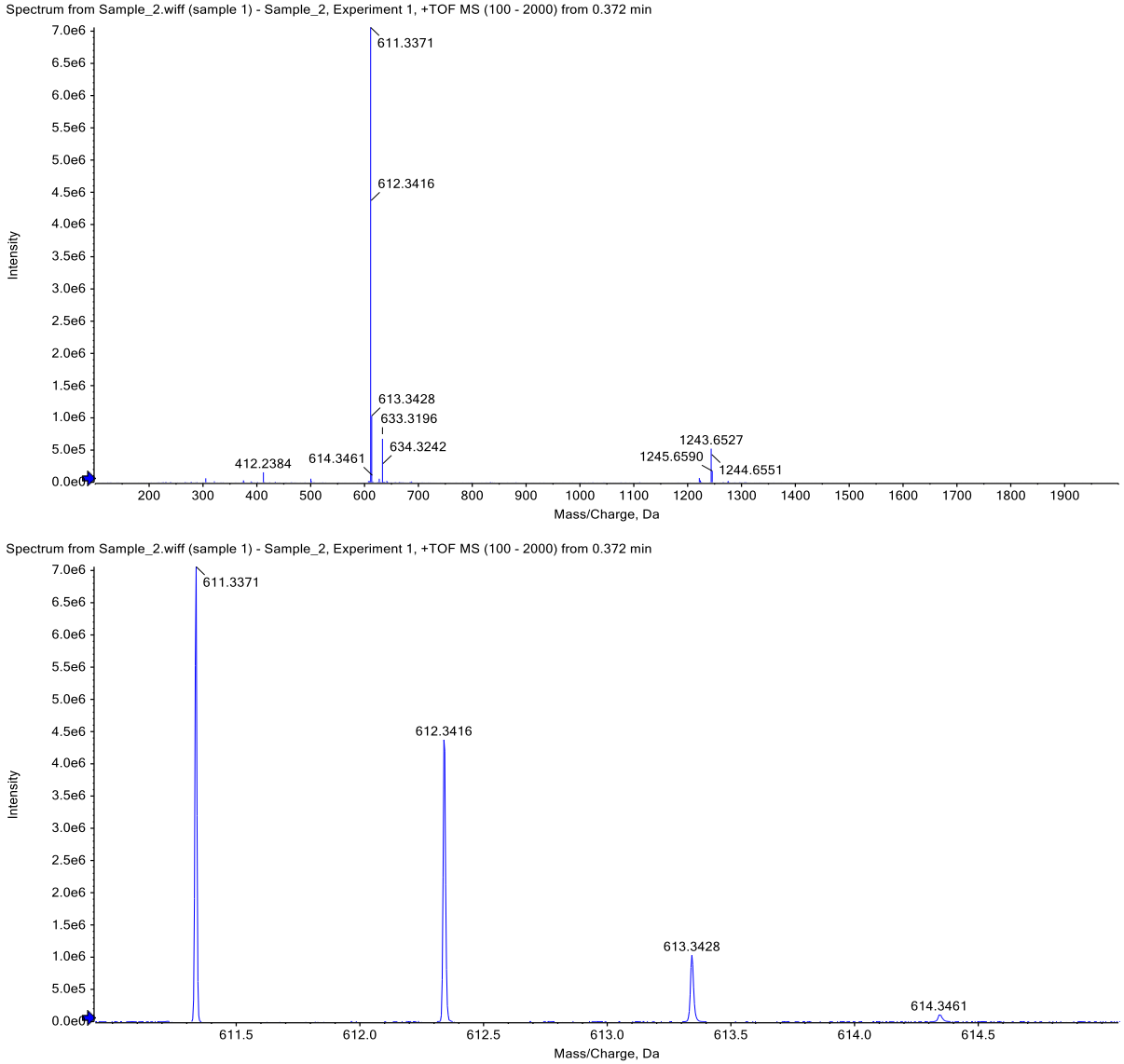

Fig. S28 HRMS spectrum and isotope distribution pattern of **Di-H**.

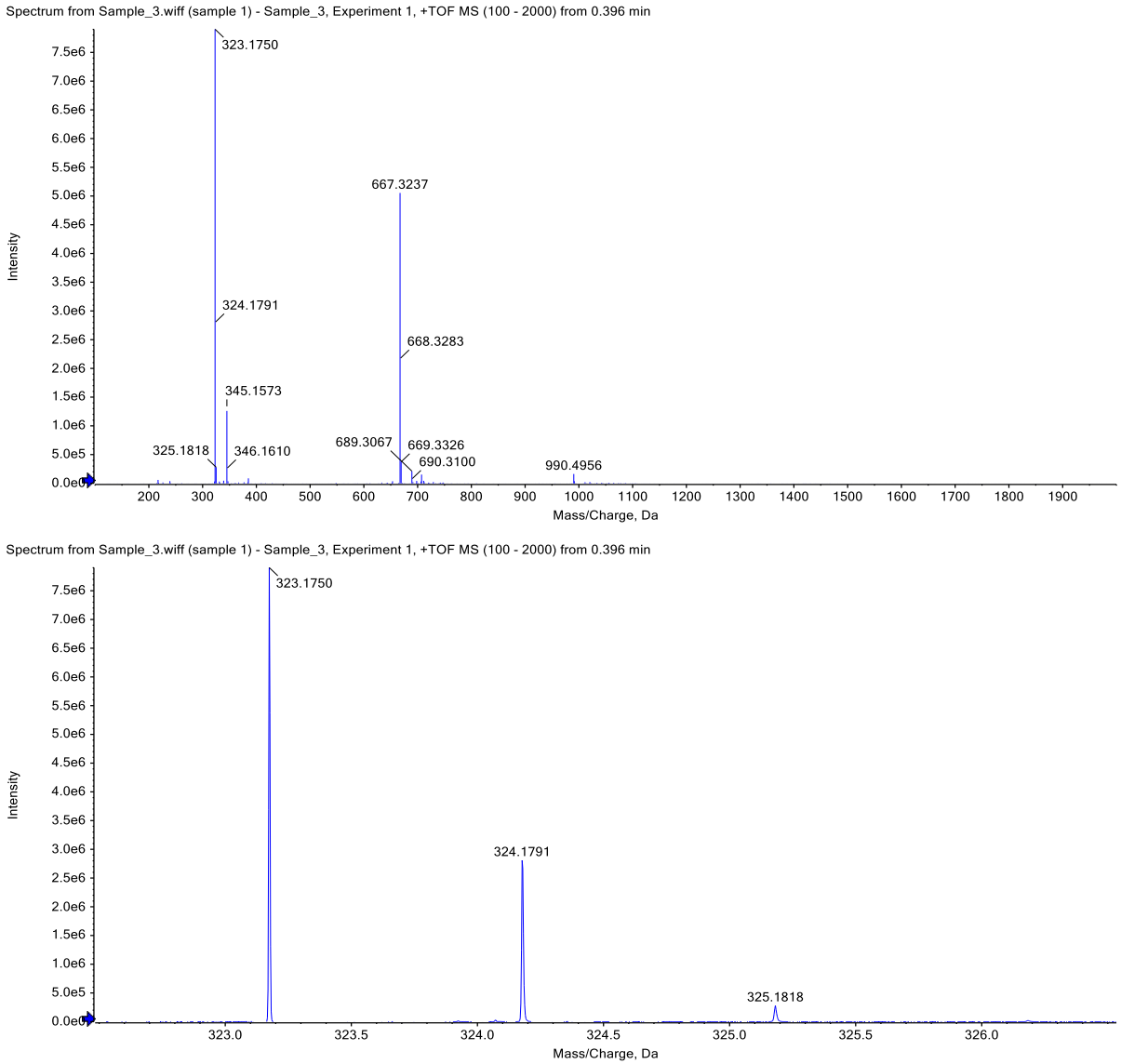

Fig. S29 HRMS spectrum and isotope distribution pattern of **Mono-OH**.

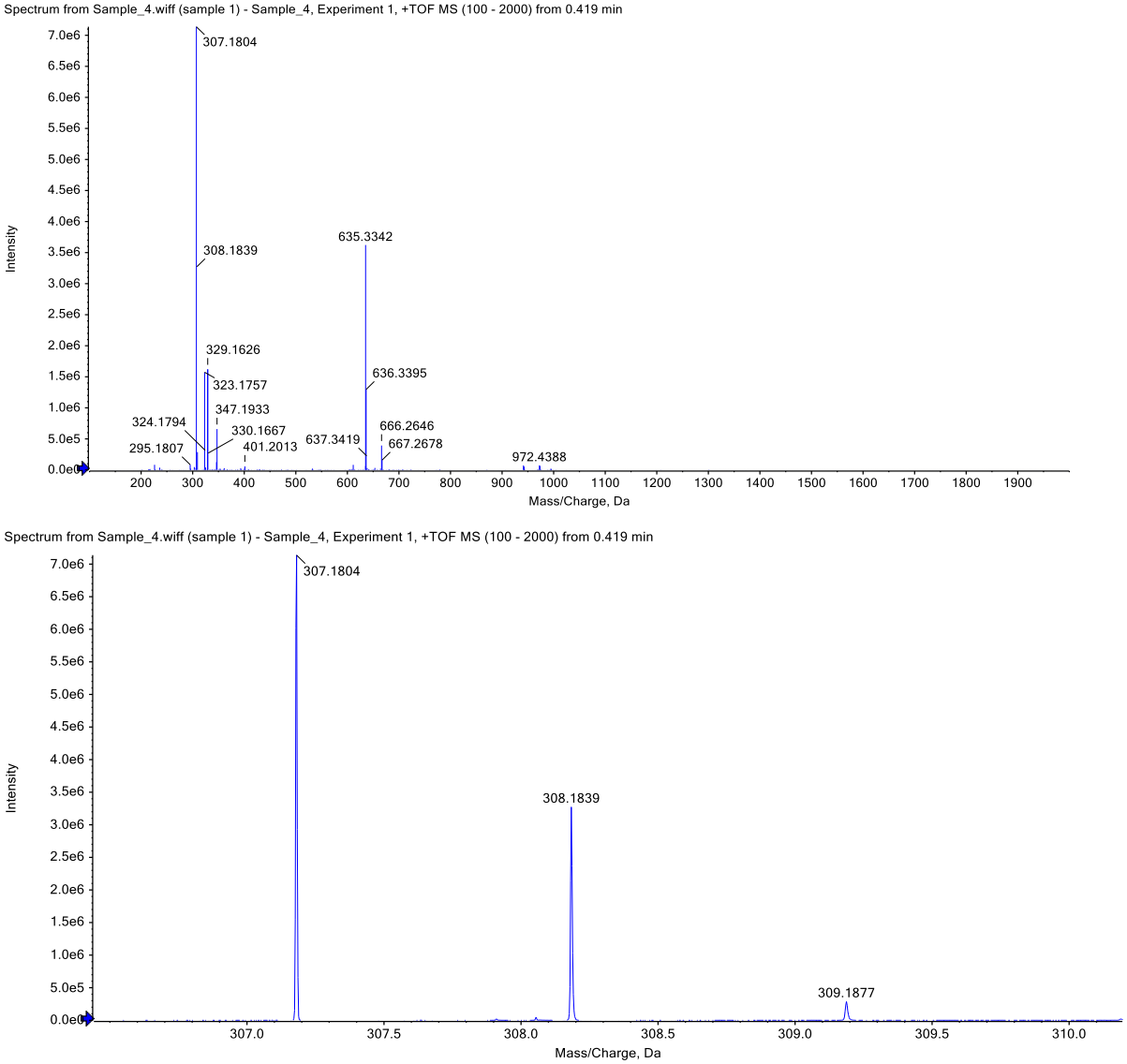

Fig. S30 HRMS spectrum and isotope distribution pattern of **Mono-H**.

S.14. Reference

[S1] C. Würth, M. Grabolle, J. Pauli, M. Spieles and U. Resch-Genger, *Nat. Protoc.*, 2013, **8**, 1535-1550.